

NEW METHOD OF INTEGRATING PERIODIC PERMANENT MAGNET (PPM) ASSEMBLY IN TRAVELING WAVE TUBES (TWTs)

T. Mulcahy and H. Song

Department of Electrical and Computer Engineering
University of Colorado
Colorado Springs, CO 80918, USA

F. Francisco

Triton Services Inc., Electron Technology Division
Easton, PA 18045, USA

Abstract—In traveling wave tube (TWT) amplifiers, an axial focusing magnetic field is required to keep electrons traveling in a narrow, pencil-like beam over the considerable length of the circuit. Conventionally, this focusing has been accomplished by using a periodic permanent magnet system housing axially polarized ring magnets. Making the structure to this point has been a complicated process consisting of brazing multiple metals together and honing the piece to the desired specifications. We present a new method of fabricating this housing structure monolithically using iron, developing magnetically oversaturated housing regions, and saving processing time and effort.

1. INTRODUCTION

The periodic permanent magnetic (PPM) configuration is a low cost, light weight alternative to the solenoid magnet electron beam confinement system commonly used in a traveling wave tube (TWT) amplifier, a high bandwidth microwave power amplifier system [1]. An example of a TWT can be seen in Figure 1. To function, thermionically excited electrons are accelerated at energies of thousands of electron volts down the hollow tube of the TWT. A helix coil, injected with a small signal RF wave is used to extract energy from electrons that are

Corresponding author: H. Song (hsong@eas.uccs.edu).

traveling down the TWT. The electric field of the small signal RF wave interacts with the electrons as they move. If the RF velocity is matched properly with the velocity of the electrons, significant amplification of input power can be realized at the output port of the helix [2].

The PPM system of the TWT is designed to keep the electron beam focused as it travels through the axis of the helix. By alternating the ring magnet polarity such that like poles are facing each other, several small containment fields of useful flux density can be created without having a single flux field with a single peak flux density toward the center of the TWT structure. In this way very mass efficient structures can be realized [3].

Figure 2 shows a simulation of the conventional manufacturing method displaying the vectored flux density field simulation using Ansoft Maxwell 2D [4].

Recently, conventional PPM stacks have been assembled using a high involvement processing routine which includes a metal brazing and subsequent honing processes. This can be time and resource intensive [5], and may be prone to unnecessary failure rates [6]. Presented here is a new method of manufacturing the PPM portion of the TWT, or integrated pole piece (IPP) input line, machining the pole pieces which house the magnets out of a single piece of iron and honing the structure to the correct tolerances. The new method decreases the time and effort required to make the PPM system, and this manufacturing can be held to very tight manufacturing tolerances. Different approaches to this axial flux field generation have also been investigated; including designs by Baird [7], an alternate PPM system to the one presented here by Hong [8] and a non-periodic permanent magnet solenoid system by Leupold [9].

In preparation for this article, a combination of simulations and measurements of conventional prototype PPM structures were performed. A description of this work will be presented after a more detailed discussion of both the conventional and new proposed integrated PPM designs. Conclusions and possible directions for future work will be presented following.

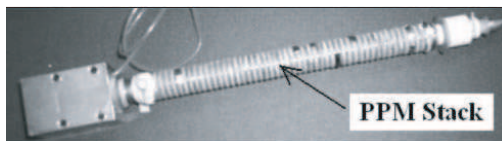


Figure 1. Triton Electron Technology Division's high frequency TWT. Periodic permanent magnet stack with brazed pole pieces are shown.

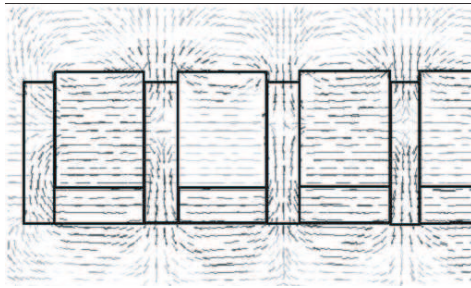


Figure 2. Vected magnetic flux density field. The lighter color indicates less magnetic flux density. The plot was generated in Maxwell 2D [4].

2. MATERIALS AND METHODS

2.1. Comparison of Conventional and New Integrated PPM Structures

The PPM portion of the helix TWT is a complicated structure designed to, among other things, maintain vacuum, contain the electron beam, house the RF helix coil, and maintain the placement of the beam confining permanent magnets system. A cross-sectional view of this system can be seen in Figure 3(a). The magnets are aligned such that they encircle a central tube through which electrons will travel down the center.

By manufacturing the magnets in a semi-cylindrical fashion, having a wall thickness, M_o minus M_i , and a cylindrical height M_t , as defined in Figure 3, setting the magnetization such that it is axially directed, the magnets can be mated around the PPM housing portion, or input line of the TWT, and clipped together. Permanent magnets made of the rare earth material Samarium Cobalt was chosen for its high coercive force (H_c) and retentivity (B_r) [10] and energy product, H_c times B_r .

As shown in Figure 3(a), the conventional input line is manufactured by brazing a series of hollow iron cylinders (pole pieces) to a corresponding set of non-magnetic (Monel) spacers, aligning the inner diameters. This configuration is then center bored and honed to specification, removing the excess material to allow placement of the RF helix structure. This is a cumbersome manufacturing process that can be easily remedied by the new process presented here.

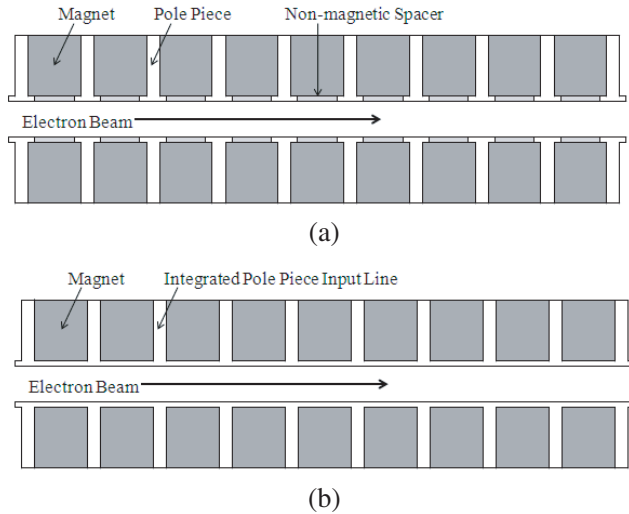


Figure 3. (a) Cross sectional view of a conventional PPM structure used in TWT and (b) proposed new PPM structure.

To address the difficulties with manufacturing the input line in the conventional sense, it has been investigated to use a single iron piece rather than brazing a set of pieces. This process requires only one major processing step to machine the proper dimensions. The material used is Carpenter Core Iron. This method of PPM construction would then use a similar process of magnet manufacture as well as having a similar magnet attachment method as the conventional process. The magnets would have dimensions modified such that the inner diameter, M_i , would mate against the outer diameter of the input line wall as seen in Figure 3(b).

Compared to conventional method, the new method reduces magnetic field at the axis since the single iron pole piece acts as a shield. It absorbs the magnetic field so only a portion of the field survives outside the shield. However, this can be overcome by adjusting dimensions of magnet and pole piece. A large number of experiments and simulations were carried out in order to investigate the viability of the new proposed method.

Figure 5 shows an example of the new method PPM input line, and Figure 6 shows how the magnets would be clipped into place. A Triton F-2456 TWT magnet system was chosen for analysis. Axial flux density measurements were taken using a conventional PPM structure made to specifications defined in Figure 4, and called out in Table 1.

Table 1. Characteristics of F-2456 conventional magnet stack.

Symbol	Quantity	Value
M_t	magnet thickness	0.085"
M_i	magnet inner diameter	0.202"
M_o	magnet outer diameter	0.420"
-	magnet material	samarium cobalt
P_t	pole piece thickness	0.030"
P_i	pole piece inner diameter	0.112"
P_o	pole piece outer diameter	0.400"
-	pole piece material	iron
H_t	hub thickness	0.000
H_o	hub outer diameter	0.000
B_{peak}	peak field	1960.5 Gauss
G_t	gap distance between hub and ring	0.00
R_t	ring thickness	0.00
R_o	ring outer diameter	0.00

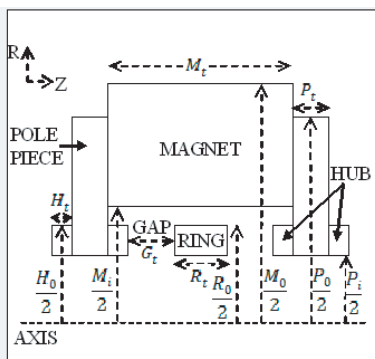


Figure 4. Cross sectional drawing of one PPM cell with dimensions referenced.

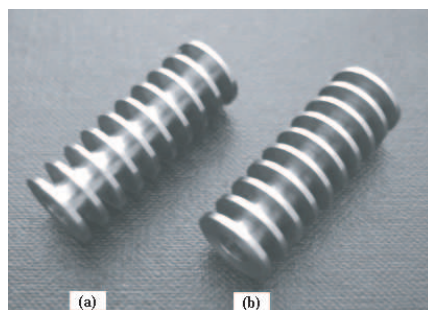


Figure 5. Integrated pole piece-shell assembly made of Consumet Core Iron for (a) 0.010 and (b) 0.015 inch thick wall.

Since the tube is made of a magnetic material, Carpenter Core Iron in this case, careful attention has to be paid to the dimensions the input line is manufactured to. Changes on the order of thousands of an inch can have a dramatic effect on the internal flux density.

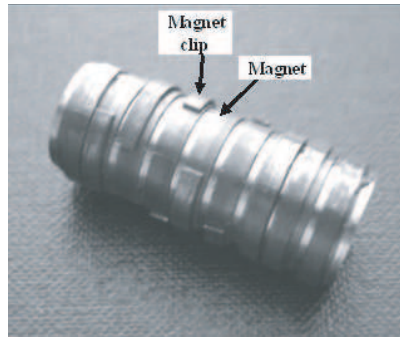


Figure 6. Integrated pole piece-shell assembly with magnets attached. Magnet clips are used to hold the magnets in place.

2.2. Simulation and Measurement

To verify that this new method would maintain the same magnetic flux fields that the conventional structure produced, two major approaches were taken. First was to measure the axial magnetic flux density of conventional structure and the three prototypes of the new method. Next, simulations were developed to validate the measurements and investigate variations in the pole piece dimensions.

Measurements were taken using a Bell 640 Gaussmeter. Data was first measured for the conventional structure. The magnets were then removed and affixed to each of the three new method prototypes. These prototypes varied from each other in that they had different input line wall thicknesses of 0.007, 0.010, and 0.015 inch respectively.

Next, the coercive force (H_c) and retentivity (B_r) properties for the conventional structure were derived using Ansoft Maxwell 2D, matching the axial magnetic flux values of the measured structure to the equivalent simulated structure. From this the equivalent 0.007, 0.010, and 0.015 inch walled input line new structures were simulated using these magnet dimensions. The Maxwell simulations showed that there were regions within the IPP walls with flux density levels of 250 kG and some regions in the IPP that were flux neutral. The saturation level for the iron used has been determined to be 16.5 kG illustrating the semi-saturated nature of this piece. Table 2 shows general dimensions used for hardware simulation.

Simulations of axial magnetic field as the magnet inner diameter (M_i) was allowed to vary to meet with the outer diameter of the input line were performed next. This simulation represents a future manufacture design. The simulated data shows that the best match for the conventional piece is obtained by using the new method with

these magnet dimensions and thickness of 0.010 inch. This match can be seen in Section 3. Most of the remaining variations were thus based off of the 0.010 inch wall structure.

Subsequent simulations include investigations into the variation of axial magnetic field distribution with variations in the coercive force (H_c) and retentivity (B_r) of the magnets, how variations of the magnet and pole piece dimensions affected axial magnetic field, the effect of iron magnet clips, and how a magnetic flux adjustment ring, would affect axial magnetic field. Table 3 shows a complete list of variations in the simulations performed.

Table 2. Simulation structure dimensions & properties.

Structure	P_t	P_o	P_i	M_t	M_o	M_i	R_t	R_i	R_o	H_c	B_r
Conventional	0.030 inch	0.200 inch	0.056 inch	0.085 inch	0.210 inch	0.101 inch	-	-	-	3.35×10^5 A/m	.435 T (4.35 kG)
.007, .010, .015 inch wall measured using Conventional structure magnets	0.030 inch	0.200 inch	0.056 inch	0.085 inch	0.210 inch	0.101 inch	-	-	-	varies	varies
.007, .010, .015 inch wall Manufacture Simulation	0.030 inch	0.200 inch	0.056 inch	0.085 inch	0.210 inch	varies	-	-	-	varies	varies
Ring Structure Base, using .010 inch Conventional structure	0.030 inch	0.200 inch	0.056 inch	0.085 inch	0.210 inch	0.101 inch	0.055 inch	0.076 inch	0.091 inch	3.35×10^5 A/m	.435 T (4.35 kG)

Table 3. Simulation variation parameters.

Dataset	Description	Dataset	Description
Conventional Measured	Measured values from conventional/brazed manufactured piece.	$B_r = 585$ (mT)	Figure 12. Conventional and New IPP $B_r = 0.585T$.
0.007 inch Wall Measured	Measured values from machined piece with 0.007 inch thick TWT wall.	$B_r = 660$ (mT)	Figure 12. Conventional and New IPP $B_r = 0.660T$.
0.010 inch Wall Measured	Measured values from machined piece with 0.010 inch thick TWT wall.	M_o 0.2225 inch	0.010 inch Future Manufacture Simulation, M_o , increased to 0.2225 inch.
0.015 inch Wall Measured	Measured values from machined piece with 0.015 inch thick TWT wall.	M_i 0.885 inch	0.010 inch Future Manufacture Simulation, M_i , decreased to 0.0885 inch.
Conventional Simulated	Simulated values from conventional/brazed manufactured dimensions.	M_t 0.100 inch	0.010 inch Future Manufacture Simulation, M_t , increased to 0.100 inch.
0.007 inch Wall Simulated	Simulated values from machined piece with 0.007 inch thick TWT wall.	M_t 0.060 inch	0.010 inch Future Manufacture Simulation, M_t , decreased to 0.060 inch.
0.010 inch Wall Simulated	Simulated values from machined piece with 0.010 inch thick TWT wall.	P_o 0.250 inch	0.010 inch Future Manufacture Simulatin, P_o , increased to 0.250 inch.
0.015 inch Wall Simulated	Simulated values from machined piece with 0.015 inch thick TWT wall.	P_o 0.125 inch	0.010 inch Future Manufacture Simulatin, P_o , decreased to 0.125 inch.
0.007 inch Future Manufacture Simulation	Simulated values from machined piece with 0.007 inch thick TWT wall, $M_i = .073$ inch.	P_t 0.050 inch	0.010 inch Future Manufacture Simulatin, P_t , increased to 0.050 inch.
0.010 inch Future Manufacture Simulation	Simulated values from machined piece with 0.010 inch thick TWT wall, $M_i = .076$ inch.	P_t 0.010 inch	0.010 inch Future Manufacture Simulatin, P_t , decreased to 0.010 inch.
0.015 inch Future Manufacture Simulation	Simulated values from machined piece with 0.015 inch thick TWT wall, $M_i = .081$ inch.	Clips	Simulated values from machined piece with 0.010 inch thick TWT wall and clips of iron.
$H_c = 335$ (A/m)	Figure 11. Conventional and New IPP $H_c = -3.35e + 005$ A/m.	Ring Structure Base	Simulated values from machined piece with 0.010 inch thick TWT wall.
$H_c = 385$ (A/m)	Figure 11. Conventional and New IPP $H_c = -3.85e + 005$ A/m.	R_o 0.096 inch	Ring Structure Base, outer diameter, R_o , increased to 0.096 inch.
$H_c = 435$ (A/m)	Figure 11. Conventional and New IPP $H_c = -4.35e + 005$ A/m.	R_o 0.086 inch	Ring Structure Base, outer diameter, R_o , decreased to 0.086 inch.
$H_c = 485$ (A/m)	Figure 11. Conventional and New IPP $H_c = -4.85e + 005$ A/m.	R_t 0.065 inch	Ring Structure Base, thickness, R_t , increased to 0.065 inch.
$B_r = 435$ (mT)	Figure 12. Conventional and New IPP $B_r = 0.485$ T.	R_t 0.045 inch	Ring Structure Base, thickness, R_t , increased to 0.045 inch.
$B_r = 510$ (mT)	Figure 12. Conventional and New IPP $B_r = 0.510$ T.		

There were some initial difficulties getting some of the simulations to converge, primarily due to meshing issues in Ansoft Maxwell 2D. To ensure convergence and good data resolution, the initial mesh conditions in general had to be subjected to a manual refinement step after the first simulation.

3. RESULTS AND ANALYSIS

Figure 7 shows the result of an mPPM [11] software simulation. Single magnet shown in Figure 4 with dimensions called out in Table 1 was simulated. The result shows an axial magnetic field curve that has a maximum value of 1960.5 Gauss.

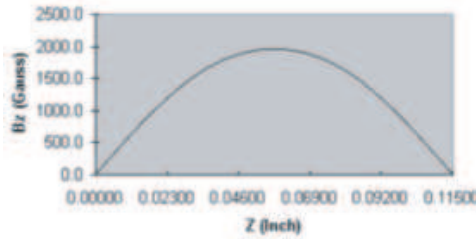


Figure 7. Simulation result of one cell Triton F-2456 conventional PPM stack employing mPPM code [11].

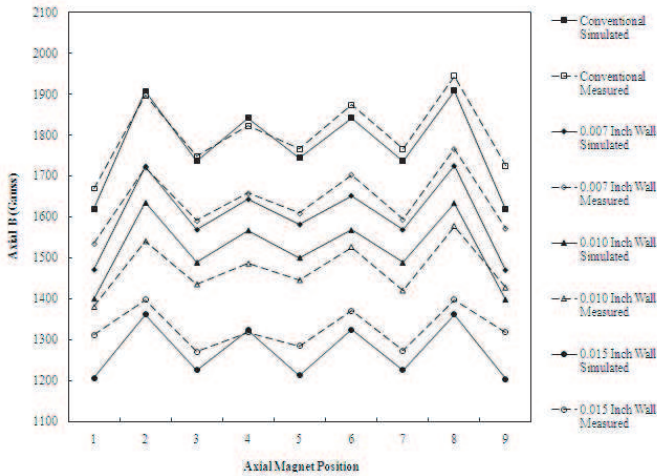


Figure 8. Comparison of measured and simulated PPM structures.

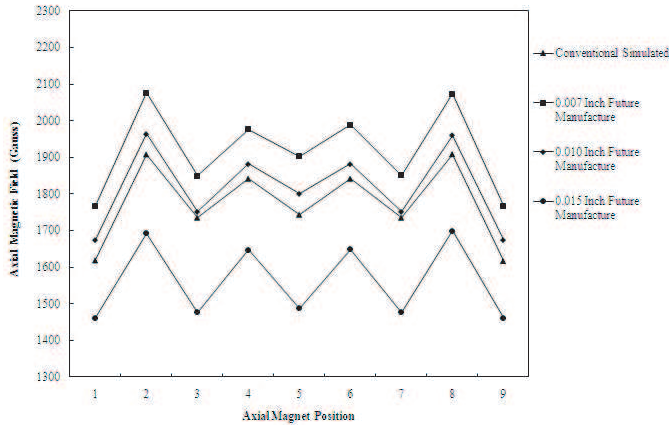


Figure 9. Simulated results of future manufacture structures.

Figure 8 illustrates the correlation between the measured and simulated data using the conventional, and 0.007, 0.010, and 0.015 inch walled measured and simulated structures. The measured data matches very well with the simulated data. The overall effect of having a reduced axial flux density using the new IPP design should be noted. The purpose of this investigation is to see the effects of the saturated input line wall thickness variation on axial magnetic field.

Figure 9 shows how the proposed new IPP manufacture would distribute the axial magnetic field. In this case the magnets would be flush against the input line wall. This shows that the best match for the conventionally manufactured PPM system is the 0.010 inch wall thick IPP system with associated magnet dimensions. This is due to the fact that these magnets would be physically larger than the magnets used to manufacture the conventional PPM system, creating a larger amount of total flux. When this larger amount of total flux is coupled with the 0.010 inch walled geometry, this provides a good match for the conventionally manufactured PPM system measurements. Referencing the good match between the conventional measured and simulated, this shows the new method is a viable alternative. Also, because of this match, the 0.010 inch new PPM system is used as the base for a majority of the remaining simulations, with exceptions noted.

Dependence of magnetic field on H_c and B_r was investigated by simulation (details shown in Table 3). This was performed in effort to show how the axial magnetic field would respond due to possible changes in magnet manufacturing lots. As expected, increasing either H_c or B_r increases the axial magnetic field. It was investigated from

these simulations that as the input line wall thickness decreases, the effects of the magnet material properties variation on the axial flux density increases. These results would be useful for failure mode investigation.

Figure 10 shows the effects of varying the magnet physical dimensions. Each case here, except for the M_t 0.060 inch, showed an increase in axial magnetic field over the simulation of the 0.010 inch new IPP with original magnet dimensions. This is to be expected because the M_t 0.060 inch case is the only case where the magnet cross section, therefore its overall volume, is smaller than that of the original version. Table 4 shows the magnet cross-sectional area for this simulation.

Table 4. Cross-sectional area of magnets for simulation shown in Figure 10.

Dataset	Area
0.010 inch future method	0.011390 inch ²
0.010 inch conventional method	0.009265 inch ²
M_o 0.220 inch	0.010115 inch ²
M_i 0.091 inch	0.010115 inch ²
M_t 0.100 inch	0.010900 inch ²
M_t 0.060 inch	0.006540 inch ²

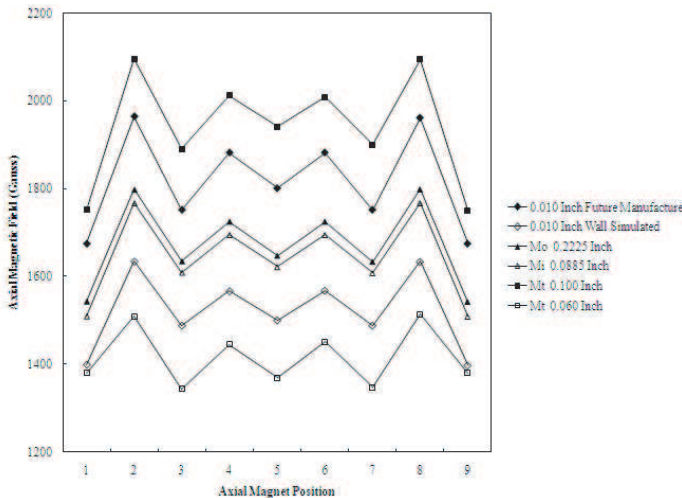


Figure 10. Simulated results of magnetic dimension variation.

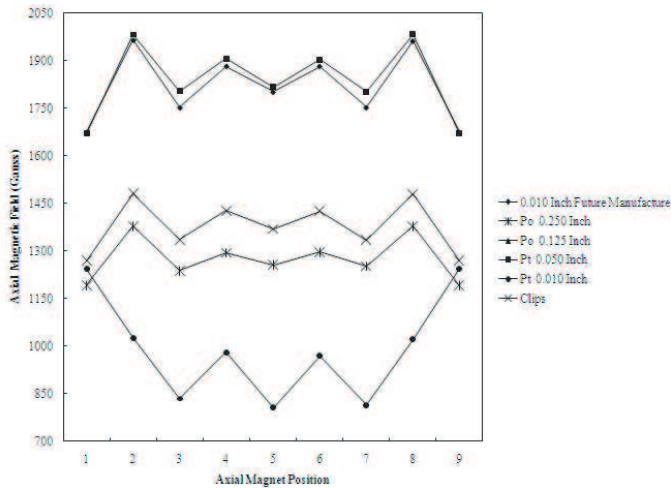


Figure 11. Simulated results of pole piece dimension variation.

The results of varying the pole piece dimensions can be seen in Figure 11. The effect of the iron’s saturation regions can be seen as the distribution and volume of the iron affects the axial magnetic field. The most interesting of this case is where the volume of iron increased in simulation $P_o = 0.250$ inch, but the axial magnetic field was reduced. In this case the flux was directed away from the axis of the PPM structure. In the case of $P_t = 0.010$ inch, the walls were too thin to develop enough flux directed into the PPM structure to match the results of the 0.010 inch future manufacture. This affected both the value and basic profile of the axial flux density distribution. As a manufacturing investigation, the affixing clips were modeled using iron as material. This last simulation was done as an investigation into possible adverse effects of using improper clip material. This simulation also had the effect of pulling down the axial magnetic field plot.

Finally, an investigation into how iron adjustment rings would affect the axial magnetic field was performed. The modeled structure was 0.010 inch thick wall shown in Figure 9 and the adjustment rings are illustrated in Figure 13. The adjustment rings were inserted into the air gap between the magnet and input line wall. Figure 12 shows the result of modeling these rings, varying the ring thickness (R_t) and ring outer diameter (R_o). As can be seen in Figure 12, insertion of this structure has a profound effect on the distribution of the flux field compared with the standard 0.010 inch structure. The overall flux magnitude has been reduced significantly. Additionally, as the ring volume is increased, the periodic high-low distribution is compromised

as can be seen in the ring base, $R_o = 0.086$ inch and $R_t = 0.065$ inch cases. The reason for this is the flux concentrated away from the center axis, into the rings. The results described in Figure 12 show that this structure also has the effect of reducing the axial magnetic flux density. The axial magnetic field varies inversely with the volume of the adjustment ring.

The above analysis shows that it is feasible to produce the same magnetic field properties with a semi-saturated integrated pole piece using this new method of PPM manufacture as the conventional method produced by adjusting the magnet and pole piece dimension and the thickness of the input line wall. With the manufacturing benefits of the new method over the conventional method, this represents a significant product improvement for the TWT manufacturing process.

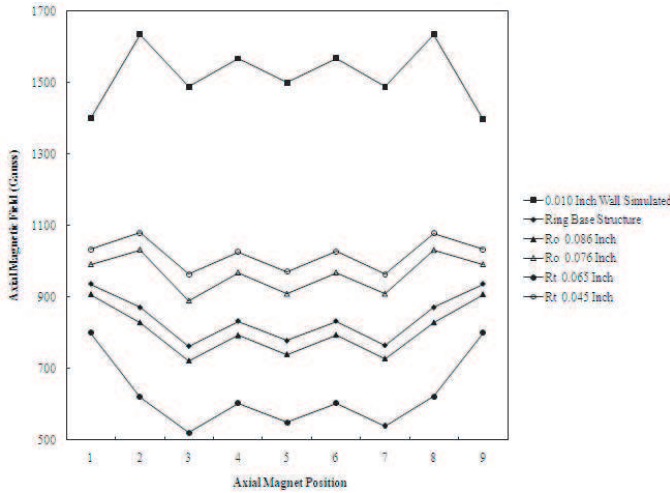


Figure 12. Simulated results of adjustment ring dimension variation.

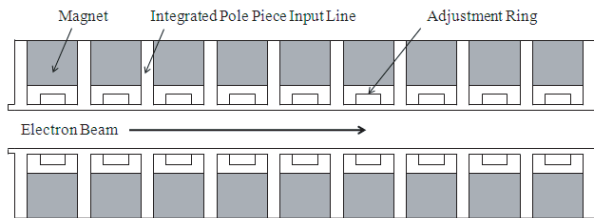


Figure 13. Cross sectional view of a conventional PPM structure used in TWT with adjustment rings illustrated.

ACKNOWLEDGMENT

This work was supported in part by the Electron Technology Division of Triton Services Inc. and the Department of Electrical and Computer Engineering of the University of Colorado at Colorado Springs.

REFERENCES

1. Leupold, H. A., "Approaches to permanent magnet circuit design," *IEEE Trans. Magn.*, Vol. 29, No. 6, 2341–2346, Nov. 1993.
2. Gilmour Jr., A. S., *Principles of Traveling Wave Tubes*, Artech House, Inc, Norwood, 1994.
3. Leupold, H. A., E. Potenziani II, and A. S. Tilak, "Iron-free permanent magnet structures for traveling wave tubes," *Proc. International Electron. Devices Meeting (IEDM)*, 411–414, 1991.
4. MAXWELL2D User's Manual, Ansoft, 2005.
5. Matsumoto, H., T. Shintake, Y. Ohkubo, H. Taoka, K. Ohhashi, and K. Kakuno, "The new fabrication method for a periodic permanent magnet (PPM) C-band (5712 MHz) Klystron," *Proc. 25th Linear Accelerator Meeting*, 14A-01, 2000.
6. Sprehn, D., G. Caryotakis, E. Jongewaard, and R. M. Phillips, "Periodic permanent magnet development for linear collider X-band klystrons," Stanford Linear Accelerator Center, Stanford University, Stanford, CA 94309.
7. Baird, J. M. and A. C. Attard, "Design of single-anode, mig-type gyrotron gun for a 35 GHz Gyro-TWT," *Microwave Symposium Digest, MTT-S International*, Vol. 81, No. 1, 261–263, Jun. 1981.
8. Zhang, H., W. Liu, S. Bai, and K. Chen, "Periodic permanent magnet focusing system with high peak field," *J. Magn. Magn. Mater.*, Vol. 320, 1675–1679, 2008.
9. Leupold, H. A., E. Potenziani II, and A. S. Tilak, "Flux tailoring of permanent magnet solenoids," *IEEE Trans. Magn.*, Vol. 29, No. 6, 2905–2907, Nov. 1993.
10. Strnat, K. J., "Modern permanent magnets for applications in electro-technology," *Proc. IEEE*, Vol. 78, No. 6, 923–946, Jun. 1990.
11. Baird, M., et al., *MPPM Program Manual User's Guide*, Apr. 2002.